Interpreting SBL data in complex resistivity regime; integration of advanced EM- techniques with existing geophysical exploration data

Lars Lorenz and Håkon Pedersen, EMGS ASA, Muralikrishna Akella, Anil Tyagi, Pranaya Sangvai and Rabi Bastia, Reliance Industries Ltd.*

Summary

SeaBed Logging (SBL) provides a powerful tool for the risk mitigation process. This study gives a case example for the application of SBL to reduce risks in drilling decisions. It underlines the importance of using all available resistivity information in the form of well logs as well as existing SBL data in the integration of the SBL data, including the interpretation of the inversion results. A discussion of the integration is performed, taking into account the uncertainties in the assumptions for different parts of the subsurface, and shows how the ranking of the prospects, based on SBL data, is interwoven with the perceived uncertainties. Drilling results yielded a commercial hydrocarbon discovery for one of the highest-ranked targets.

Introduction

Exploration in the Krishna-Godavari (KG) Basin at the East Coast of India by Reliance and other oil companies yielded several world-class oil and gas discoveries. The basin is characterized by a wide range of depositional settings, ranging from coastal plains, deltas and shelf-slope aprons to deep-sea fans. Commercial accumulations of hydrocarbons occur in sediments of Permian to Pliocene age. The most significant hydrocarbon potential, and currently targeted prospective play type, can be found in the tertiary channel–levee–overbank sediments of Mio- to Pliocene age in deep waters.

Reliance has large acreage in the KG Basin with most areas in water depths beyond 200 m. This required mitigating the risk before drilling due to the significant associated costs. For this purpose, Reliance employed SBL to identify high-resistive thin beds, a common characteristic of hydrocarbon reservoirs. Successful SBL application to targets in the Pleistocene and Pliocene interval (Tyagi et al., 2008) and refinement of the resistivity information for the area based on the interpretation of the existing SBL data, encouraged targeting of deeper intervals in the area as well.

Method

A detailed description of the SBL technique is provided by Eidesmo et al. (2002) and Ellingsrud et al. (2002). A low frequency electromagnetic signal is emitted by a horizontal electric dipole into the seabed and underlying sediments. The electromagnetic field diffuses through the sediment column and is rapidly attenuated due to low resistivitiy of saline pore fluids. If the field encounters a high-resistive layer and enters it at a critical angle of incidence, the energy is guided along the layer with a significantly smaller degree of attenuation and is constantly refracted back to the seafloor where it is recorded by electromagnetic receivers (Kong et al., 2002). The detection of this guided and refracted energy is the basis of SBL (Ellingsrud et al., 2001).

Background Information for the Survey Area

The prospects in the survey area are characterized by a wide range of burial depths, ranging from targets in the Late Pliocene to the Early Miocene (Figure 1). Wells drilled in the channel-levee complex of the Pleisto-Pliocene section encountered reservoir sands with thicknesses varying from few millimeters to 60 m. Depending on reservoir thickness, the reservoir resistivities were highly variable as well.

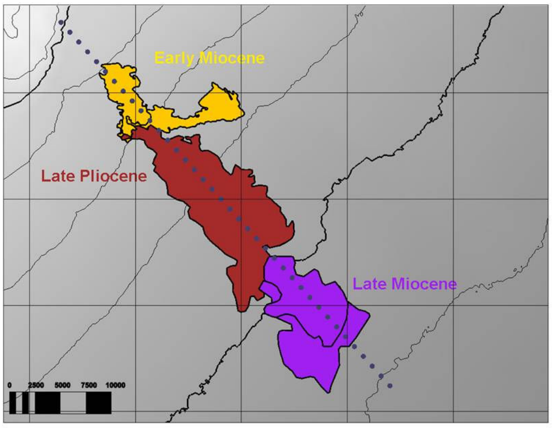

Figure 1: Survey Map with prospect polygons at different stratigraphic intervals. Prospect polygons in color, receiver positions as grey circles.

The shale resistivity as measured by the standard logging suite is normally around 0.7-0.9 ohmm. Interpretation of previously collected SBL data in the Krishna Goddavari Basin (Tyagi et al., 2008, Suffert et al., 2008), as well as available anisotropy logs indicated a higher vertical resistivity, about 1.5 to 2.0 times higher than the horizontal resistivity.

While the higher background resistivity improved the ability to inject currents in the deeper section of the subsurface due to lower attenuation, it helped in a very limited manner to address the high variability of the reservoir resistivities which even for the vertical resistivity as measured by anisotropy logs could be as low as 5 ohmm. Therefore, a careful assessment of the survey parameters had to be performed.

Pre-survey modeling and survey parameters

Pre-survey modeling was performed for the diverse prospects to evaluate the sensitivity of SBL in the different target intervals. Uncertainties existed for the background resistivity of the deeper Miocene interval. Even though SBL measurements for calibrating the resistivity of this interval were in principle available through other surveys in the area, there were uncertainties regarding how representative those measurements were.

It was therefore decided to extrapolate the Pliocene resistivities to the deeper section. Even though not ideal, 1D modeling suggested that this was a pessimistic assumption. While the predicted response for the higher resistive Early Miocene reservoirs was not strongly affected by the slightly lower resistivity contrast, the frequency range with sensitivity to these deeper targets was significantly lower.

The following 3D feasibility study suggested that detectable responses could be recorded from the different targets. On the other hand, the frequencies with the highest sensitivity were spread out widely across the frequency band due to the different target depths (Figure 2). It was therefore decided to acquire the survey by two source tows with two frequency spectrums to allow for a large enough frequency range with sensitivity to the targets for reliable inversion results.

A receiver spacing with 1.25 km was chosen to ensure sufficient data coverage for follow-up inversion of the data, and the survey line placed as centrally as possible over all the prospects, as this yielded the highest response in the pre-survey modeling (Figure 1).

Survey Results

Utilizing relative responses with the associated attributes normalized magnitude (NMvO) and phase difference (PDvO), indicated the presence of local resistive features in the shallow and deep sections of the subsurface. A significant increase in the complexity of the resistivity regime in the deeper section towards larger water depths was observed as well. Figure 3 illustrates this behavior by comparing the response of short source-receiver offsets of a higher frequency, measuring the resistivity distribution of the shallow subsurface, and the response of large source-receiver offset of a low frequency, probing a much deeper interval.

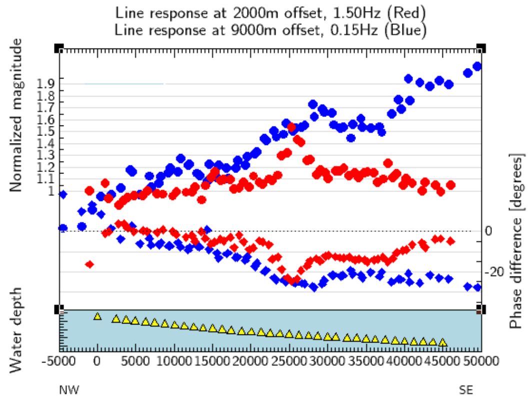

Figure 3: NMvO and PDvO attribute responses at high frequency – low offset and large offset – low frequency in comparison, illustrating the presence of local resistors as well as an increasing complexity in the resistivity regime with depth.

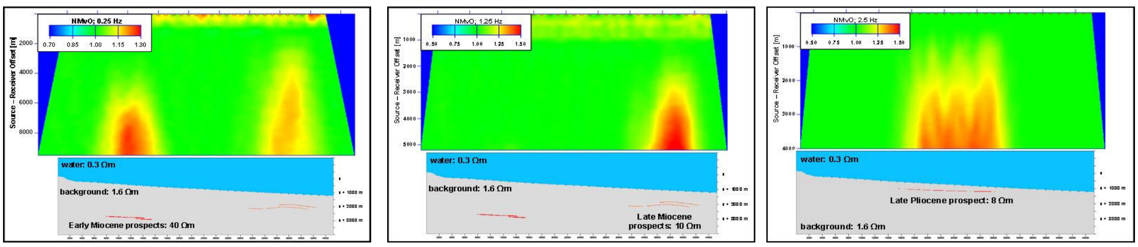

Figure 2: Predicted NMvO responses for the different target intervals at the frequencies with highest sensitivity to the respective target. Only data above the anticipated noise floor is presented. Models for the respective targets are presented together with the response.

To address this complexity in the resistivity regime and to progress from a qualitative to a quantitative analysis of the measurements, 3D inversion of the data was performed. The 3D inversion algorithm is described in more detail by Zach et al. (2008) and Støren et al. (2008).

The 3D inversion result with a half-space starting model is shown in Figure 4. The shallow section is dominated by a local increase in resistivity in the middle of the line. In the deeper section, one can observe an isolated resistor to the NW and an increase in resistivity in the Miocene and Eocene interval towards SE.

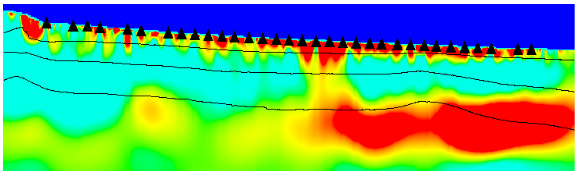

Figure 4: 3D inversion result with a Half-space starting model. Receivers included in the inversion are spatially placed as black triangles. Miocene and Eocene intervals are marked for reference purposes.

To address the non-uniqueness of the inversion result as well as the smoothness constraint in a gradient-based inversion scheme, additional seismic information had to be used to evaluate different resistivity models. The seismic information was incorporated in 3D forward models, and combined with an interpretation of the 3D inversion results to describe the resistivity framework.

Figure 5 shows a resulting background model which describes well the response in the calibration areas without including significant resistivity changes in the Early Miocene, indicated by the 3D inversion result. This interpretation of the 3D inversion results was based on the absence of high resistivities in representative well logs, probing the Miocene section. The presence of prospects in this interval were considered as possible solutions for the higher resistivities, causing together with the smoothness constraints of the gradient-based inversion scheme, the appearance of a thick resistive sedimentary layer.

To address the residual data misfit, thin resistors as typical representation of reservoirs were then introduced at the different prospect intervals. Figure 6 shows the resulting resistivity model for this realization, together with the data misfit. Numerous thin resistors were necessary to explain the residual data misfit outside of the calibration area.

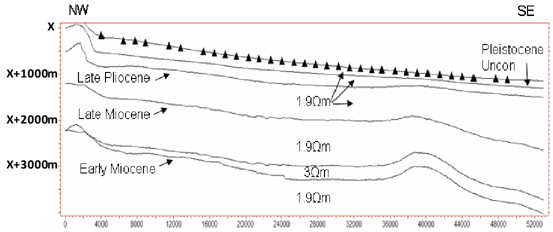

Figure 5: Background Resistivity Model, resulting from the interpretation of 3D inversion results, combined with well log information and seismic input, providing the resistivity framework for further analysis.

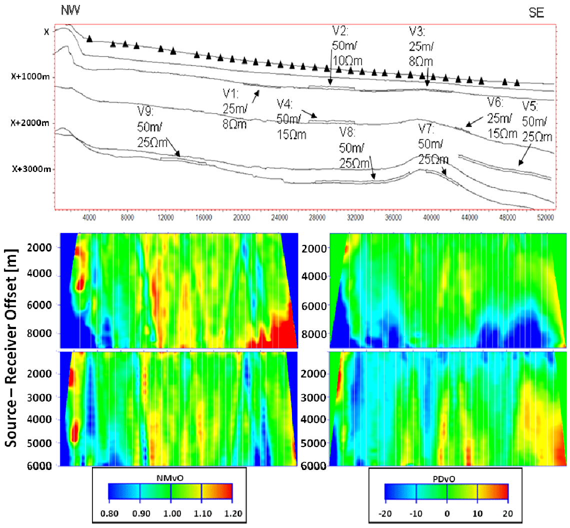

Figure 6: Final resistivity model, resulting from the interpretation of the 3D Inversion results, based on the resistivity framework in Figure 4. On the bottom, data misfit for a low and a high frequency for magnitude (left) and phase (right), displayed as direct comparison between synthetic data and measured data using NMvO and PDvO.

Discussion and Results

SBL interpretation always deals with a non-unique problem and a low frequency data set. This results in several models being able to explain the data. To truly use the interpreted resistive features, e.g. thin resistors, for risk mitigation it is necessary to evaluate how robust they are with respect to the uncertainties within the available information. As the background model provides the resistivity framework, defining how much of the excess response can be distributed towards more local features, a higher uncertainty in the background model will result in a higher uncertainty for the interpretation of thin resistors.

In the current case, the highest uncertainty is related to the resistivity of the Miocene sediments in water depths beyond 2000 m. No anisotropy well logs are available at this water depth and SBL data with sufficient sampling for this interval measures across areas with prospects, yielding very limited calibration points. In addition, structural changes in the subsurface are occurring in this area as well, amplifying the influence of an incorrect resistivity framework.

The shallow Pliocene and Pleistocene section yields the lowest uncertainty. Numerous anisotropy well logs are available, and good sampling of this interval by SBL data as calibration points is provided. Additionally, the background resistivity is at the upper end of what is expected for this interval, allowing for an increase in the resistivity of the additional features (thin resistors), while a decrease would require this area to be characterized by significantly altered resistivities compared to the surrounding areas.

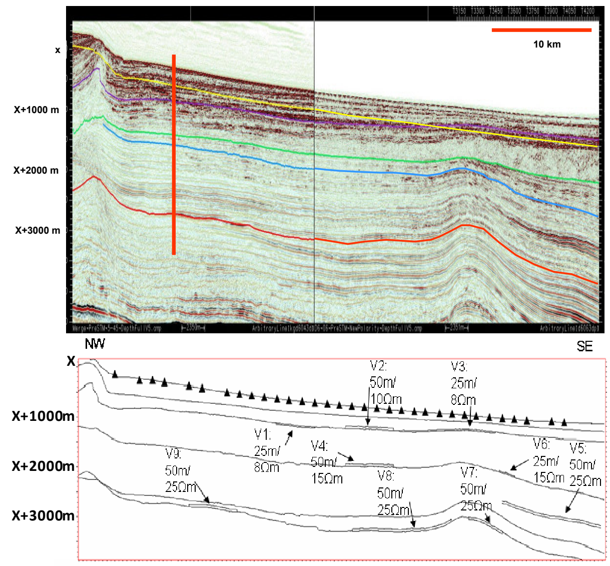

Figure 7: Seismic cross- section, displaying the position of the discovery well combined with the final 3D modeling result for comparison.

An exception for the Miocene section is the thin resistor denoted as V9. This resistor is characterized by an anomaly which is laterally limited in extension and clearly separated from the overall resistivity trend for the deeper section in standard attributes as well as in the inversion results. A very good lateral correlation exists between the prospect as defined by seismic data and the boundaries of the resistive feature. No other geometrical features (e.g. structures, pinch outs, thickness variations) with local character are indicated by the seismic, additionally reducing the likelihood of erroneous background resistivities to be the cause of the anomaly.

These considerations resulted in the recommendation to rate the shallow targets, as well as the V9 anomaly for the Miocene section, higher than the Miocene resistors in the SE part of the line. Re-evaluation of the Miocene resistors in the SE part of the line was recommended as soon as more additional data (well logs or SBL data) was available. The subsequent drilling of the V9 anomaly resulted in the discovery of a commercial hydrocarbon accumulation (Figure 7). Reinterpretation of the line is currently ongoing.

EDITED REFERENCES

Note: This reference list is a copy-edited version of the reference list submitted by the author. Reference lists for the 2009 SEG Technical Program Expanded Abstracts have been copy edited so that references provided with the online metadata for each paper will achieve a high degree of linking to cited sources that appear on the Web.

REFERENCES

Eidesmo, T., S. Ellingsrud, L. M. MacGregor, S. Constable, M. C. Sinha, S. Johansen, F. N. Kong, and H. Westerdahl, 2002, Sea bed logging (SBL), a new method for remote and direct identification of hydrocarbon filled layers in deepwater areas: First Break, **20**, 144–152.

Ellingsrud, S., M. C. Sinha, S. Constable, L. M. MacGregor, T. Eidesmo, and S. Johansen, 2002, Remote sensing of hydrocarbon layers by sea bed logging (SBL): Results from a cruise offshore Angola: The Leading Edge, **21**, 972–982.

Johansen, S. E., H. E. F. Amundsen, and T. A. Wicklund, 2007, Interpretation example of marine CSEM data: The Leading Edge, **26**, 348–354.

Kong, F. N., H. Westerdahl, S. Ellingsrud, T. Eidesmo, and S. Johansen, 2002, Seabed logging: A possible direct hydrocarbon indicator for deepsea prospects using EM energy: The Oil and Gas Journal.

Støren, T., J. J. Zach, and F. A. Maaø, 2008, Gradient calculations for 3D inversion of CSEM data using a fast finite-difference time-domain modeling code: 70th Annual Conference and Exhibition, EAGE, Extended Abstracts.

Suffert, J., P. Sangvai, F. Roth, A. Tyagi, and R. Bastia, 2008, Frontier exploration by electromagnetic scanning—A deep water example: 78th Annual International Meeting, SEG, Expanded Abstracts, 662–666.

Tyagi, A., A. Muralikrishna, L. Lorenz, H. F. E. Amundsen, and R. Bastia, 2008, De-risking exploration prospects using controlled source electromagnetic surveys: 78th Annual International Meeting, SEG, Expanded Abstracts, 702–705.

Zach, J. J., A. K. Bjørke, T. Støren, and F. A. Maaø, 2008, 3D inversion of marine CSEM data using a fast finite-difference time-domain forward code and approximate Hessian-based optimization: 78th Annual International Meeting, SEG, Expanded Abstracts, 614–618.